Eur. Phys. J. D **30**, 163–169 (2004)
DOI: 10.1140/epjd/e2004-00083-5

THE EUROPEAN PHYSICAL JOURNAL D

Efficient long-term laser excitation of a collimated beam of potassium atoms on the D2 line

A. Gopalan[1], E. Leber[1], J. Bömmels[1], S.P.H. Paul[1], M. Allegrini[2], M.-W. Ruf[1,a], and H. Hotop[1,b]

[1] Fachbereich Physik, Universität Kaiserslautern, 67653 Kaiserslautern, Germany
[2] Dipartimento di Fisica Enrico Fermi, Via Buonarotti 2, 56127 Pisa, Italy

Received 10 March 2004
Published online 29 June 2004 – © EDP Sciences, Società Italiana di Fisica, Springer-Verlag 2004

Abstract. With the aim to provide a reliable scheme for efficient laser excitation of the potassium D2 line over long periods of time, we have developed a robust stabilization of a single mode laser of frequency $f_0 = (f_{12} + f_{23})/2$ onto a crossover peak in the saturation spectrum of the ^{39}K(D2) line ($4s\ ^2S_{1/2}, F \rightarrow 4p\ ^2P_{3/2}, F'$). The two hyperfine transitions $F = 1 \rightarrow F' = 2$ (frequency f_{12}) and $F = 2 \rightarrow F' = 3$ (frequency f_{23}) are simultaneously excited by the first order sidebands $f_\pm = f_0 \pm f_{EOM}$ of the laser beam (f_0), generated by its electro-optical modulation at the frequency $f_{EOM} = (f_{12} - f_{23})/2$. In this way stable excitation of the two transitions on their proper frequencies is achieved and hyperfine pumping compensated.

PACS. 39.30.+w Spectroscopic techniques – 32.80.Bx Level crossing and optical pumping – 42.60.Fc Modulation, tuning, and mode locking

1 Introduction

The use of continuous wave (cw) single-mode or few mode lasers has been essential for a wealth of collision experiments involving laser-excited and laser-selected atoms and molecules [1–4]. One of the technical problems in such measurements is the long-term frequency stabilization of the laser [5,6] onto the atomic or molecular transition. On a short time scale, the laser is typically locked to a transmission fringe of a suitable optical cavity such as a Fabry-Perot interferometer, thus providing (in a typical dye or titanium:sapphire laser) a short-term frequency width of about 1 MHz or somewhat better. Over minutes or hours, often required for sophisticated collision experiments, standard-type reference cavities (as found in commercial cw lasers) are found to drift by intolerable amounts (>50 kHz s^{-1}), unless the cavity is long-term stabilized. The latter approach is possible with reference to, e.g., some appropriate atomic transition frequency [7], but often not easy to achieve. Another approach may involve the use of an intrinsically stable reference cavity fabricated from a low-expansion material [5,6]; the realization requires special care in acoustic decoupling and in general involves offset-locking techniques. As an alternative, direct long-term stabilization to the atomic or molecular transition frequency of interest may be applied by means of an auxiliary set-up. Although stabilization schemes involving the Doppler-broadened profile have been demonstrated [8–10], it is preferable for a reliable and accurate stabilization (as relevant for transverse excitation of an atomic or molecular beam) to use a scheme which involves the Doppler-free transition. For this purpose, signals obtained by laser excitation of an atomic or molecular beam may be used [11,12]. Alternatively, several variants of Doppler-free saturation spectroscopy involving gas cells have been shown to be well suited [5,6]. For example, our group has exploited Lamb-dip stabilized saturation spectroscopy in rare gas atom discharges for efficient long-term stabilized excitation of metastable Ne*($3s\ ^3P_{2,0}$) [13] and Ar*($4s\ ^3P_{2,0}$) [14] atoms.

In connection with the development and long-term use of an improved laser photoelectron source [15], we recently met the need to efficiently excite the potassium D2 resonance line, i.e. the transition K($4s\ ^2S_{1/2}$, $F \rightarrow 4p\ ^2P_{3/2}$, F'). In view of the natural isotopic composition of potassium, ^{39}K (about 93%) is the isotope of choice for use in beam experiments which require substantial amounts of sample. Unfortunately, the ^{39}K nucleus has a small magnetic moment, and the hyperfine structure separations are thus small [16] (see Fig. 1). Excitation of the favourable K($4s\ ^2S_{1/2}$, $F = 2 \rightarrow 4p\ ^2P_{3/2}$, $F' = 3$) transition (the excited state can only decay back to the pumped level) is easily possible with single-mode lasers at 766.7 nm, as exploited and demonstrated, e.g., in beam experiments [17]. At a natural linewidth of 6 MHz, however, hyperfine pumping involving transitions to the

[a] e-mail: ruf@physik.uni-kl.de
[b] e-mail: hotop@physik.uni-kl.de

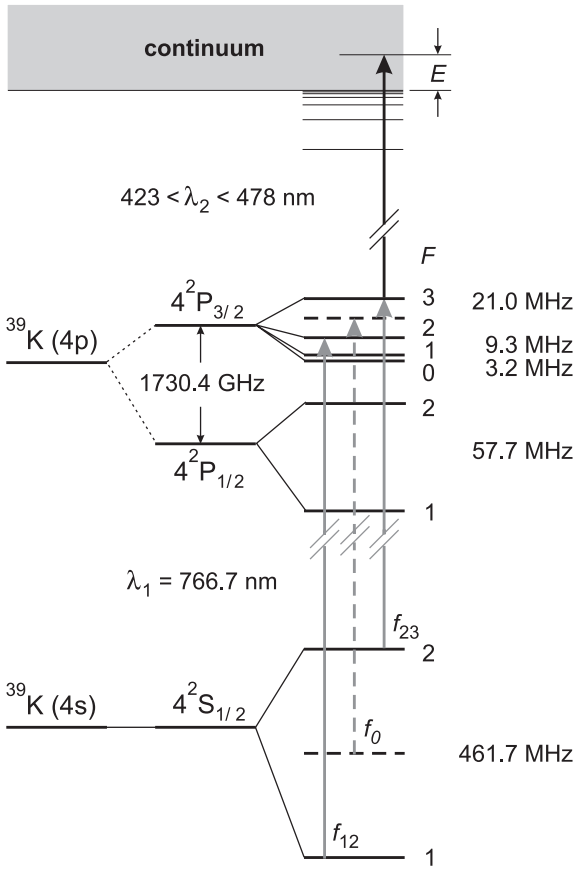

Fig. 1. Level diagram illustrating the two-step photoionization scheme of ^{39}K($4s\ ^2S_{1/2}$, F) atoms via the ^{39}K*($4p\ ^2P_{3/2}$, F') excited states. Note that *both* hyperfine states $F = 1$ and 2 in the ground level participate in the optical pumping process; they are excited to the hyperfine states $F' = 2$ and 3, respectively, at the relevant transition frequencies f_{12} and f_{23}. These two frequencies are prepared as the (±) 1st order sidebands of a single frequency laser ($f_0 = (f_{12} + f_{23})/2$) passing through an electro-optical modulator (EOM), driven at the frequency $f_{EOM} = (f_{12} - f_{23})/2 = 220.35$ MHz. The frequency f_0 is actively long-term stabilized by crossover saturation spectroscopy. The numbers in the right column indicate the energy separation [MHz] between adjacent F-levels.

close-by K*($4p\ ^2P_{3/2}$, $F' = 2$) level (followed by spontaneous decay to the unpumped K($4s\ ^2S_{1/2}$, $F = 1$) level) is a serious issue [1,2,4], especially at laser intensities sufficient to reach a substantial quasi-stationary population in the excited level. This problem can be solved by simultaneous excitation of the two transitions K($4s\ ^2S_{1/2}$, $F = 2 \rightarrow 4p\ ^2P_{3/2}$, $F' = 3$) (frequency f_{23}) and K($4s\ ^2S_{1/2}$, $F = 1 \rightarrow 4p\ ^2P_{3/2}$, $F' = 2$) (frequency f_{12}), using two laser frequencies separated by $f_{12} - f_{23} = 440.7$ MHz (see Fig. 1).

There are different technical approaches to realize such a two-frequency excitation scheme [4]. One option consists in using two independent lasers [18], stabilized to the relevant transition frequencies. Alternatively, one may design a laser in a special way such that the output consists of two frequencies with the desired frequency difference [19,20]. A third option involves a frequency-shifting method with an acousto-optical modulator [4–6], as applied to two-frequency excitation of ^{6}Li atoms [21] and ^{23}Na atoms [22]. In another approach, sidebands are produced by means of an electro-optical phase modulator (EOM) [4–6,23,24]. The pair of first order sidebands has been used for two-frequency excitation of ^{23}Na atoms [25–27]; as an alternative, the carrier frequency and the positive first order sideband at doubled modulation frequency have been applied, but this scheme was found to be somewhat less effective [26]. More recently, the latter approach was also exploited for two-frequency excitation of ^{6}Li [28] and ^{39}K [29].

In the present work, two-frequency excitation of ^{39}K atoms is realized by means of the two EOM produced first order sidebands of a long-term stabilized single mode laser. We use a resonance modulator similar to that described previously in connection with efficient excitation of the sodium D2 line [24,25], but modified to allow operation at the modulation frequency $f_{EOM} = (f_{12} - f_{23})/2 = 220.35$ MHz. When a single frequency laser, run at and stabilized to the frequency $f_0 = (f_{12} + f_{23})/2$, is subjected to electro-optical modulation f_{EOM}, the first positive and negative sidebands $f_\pm = f_0 \pm f_{EOM}$ of the resulting frequency spectrum are identical with the transition frequencies f_{12} and f_{23}, respectively. Correspondingly, the EO-modulated laser should allow efficient excitation of the potassium D2 line. The main problem addressed in this paper is how to realize a robust long-term frequency stabilization of this laser to the atomic transition. The basic idea is to exploit stabilization of the single-mode laser (f_0) to a crossover peak present in the saturation spectrum of the potassium D2 line.

The paper is organized as follows. In Section 2 we present the experimental set-ups. In Section 3 we demonstrate the problem of hyperfine pumping in the K(D2) line as well as the usefulness of the proposed EOM sideband excitation scheme by measuring the efficiency for two-step photoionization via the K*($4p\ ^2P_{3/2}$) level with both a single mode and the EO modulated excitation laser. In Section 4, we present the Doppler-free saturation spectrum of the K(D2) line, dwell on the origin of the crossover peak relevant for long-term laser stabilization of the single mode laser (f_0) and discuss the performance of the long-term stabilization. In Section 5, we conclude by mentioning recent applications of the EOM sideband excitation for studies of the polarization dependent photoionization cross-section of K*($4p\ ^2P_{3/2}$) atoms and for efficient laser photoelectron production by ionizing K*($4p\ ^2P_{3/2}$) atoms with an intracavity dye laser at wavelengths below 455 nm.

2 Experimental set-ups for two-step photoionization and long-term laser stabilization

In the test experiments described in Section 3 the quasi-stationary population of excited ^{39}K*($4p\ ^2P_{3/2}$, F') atoms, produced by transverse, nearly Doppler-free

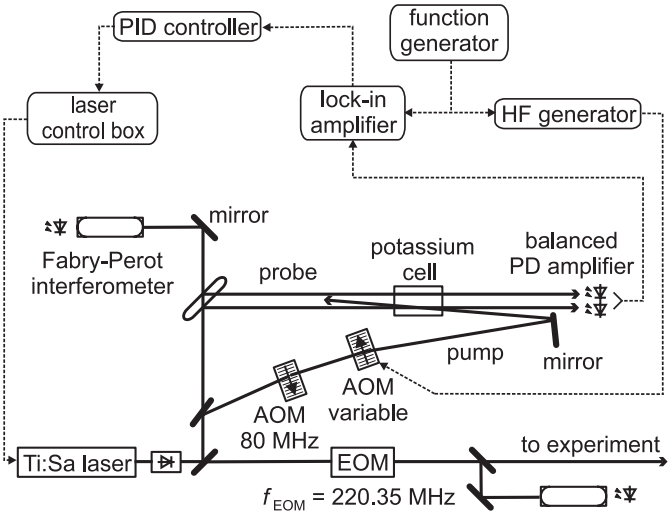

Fig. 2. Set-up used for long-term stabilization of the Ti:Sa laser with frequency $f_0 = (f_{12} + f_{23})/2$ by means of crossover saturation spectroscopy with ^{39}K atoms in a vapour cell (see text for details).

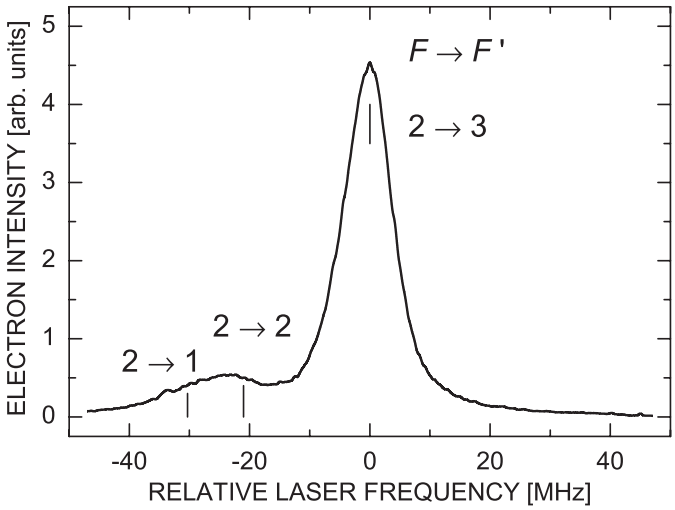

Fig. 3. Excitation spectrum of the ^{39}K(D2) line using a single-mode laser with an intensity of about 2 mW cm^{-2} (power of probing photoionization laser 60 mW ($\lambda_2 = 453$ nm)).

excitation of a collimated beam of potassium atoms by a continuous wave (cw) laser beam (wavelength λ_1), is probed by one photon ionization with a cw laser of sufficiently short wavelength ($\lambda_2 < 455$ nm) [30]. The photoionization apparatus will be described in some detail in a future paper in which we shall present energy- and polarization dependent total and angle-differential photoionization cross-sections of aligned laser-excited ^{39}K($4p_{3/2}$) atoms. Briefly, a beam of potassium atoms (mean velocity 600 m s^{-1}, full collimation angle 0.007 rad, residual Doppler width for the D2 line 2.7 MHz) is formed by a differentially pumped two-chamber oven. Typical K($4s$ ^{2}S$_{1/2}$) densities in the photoionization region are around 10^8 cm^{-3}. The atomic beam is modulated by a mechanical chopper. The excited state population may be monitored by synchronous detection of the K(D2) fluorescence with a photodiode followed by a lock-in detector. In the present work, however, the background-free photoionization detection of the excited state density was preferred. The photoionization chamber is made of mumetal coated with colloidal graphite, thus achieving low residual electric fields (<0.5 V m^{-1}) and magnetic fields (<5 × 10^{-7} T). In the test experiments presented in Section 3, photoions or photoelectrons were extracted from the ionization region by a suitable electric field and detected with a CuBe electron multiplier, followed by an amplifier and a lock-in detector.

The experiments in Section 4 were carried out with a set-up for Doppler-free saturation spectroscopy which is sketched in Figure 2. It involves a potassium cell heated to about 353 K (vapour pressure about 3.6×10^{-6} mbar), a saturating laser beam ("pump", typical power 10 mW, beam diameter 1 mm), and two parallel 'probe' beams of nearly equal power around 1 mW (separation about 10 mm, diameters equal to that of pump beam) with one of them (nearly) anticollinear to the pump beam. The two probe beams are sampled by a pair of balanced detectors [31].

A frequency offset between the frequencies of the probe laser (f_{pr}) and the pump laser (f_{pu}) may be introduced by passing the pump laser through a pair of acousto-optical modulators (AOM). The first AOM (operated in the +1st diffraction order, thus raising the laser frequency by $+f_{AOM1}$) is driven by the fixed frequency f_{AOM1} = 80 MHz while the second AOM (operated in the –1st diffraction order) is driven at the frequency f_{AOM2} = 80 MHz or 110 MHz. Normal Doppler-free saturation spectroscopic measurements are carried out with identical AOM frequencies while the other option is used for long-term stabilization of the Ti:Sa laser onto a crossover of the K(D2) line (see Sect. 4).

3 Demonstration and compensation of hyperfine pumping in the K(D2) line

The experiments described in this section were carried out with the photoionization apparatus, briefly introduced in Section 2. To set the scene, we first show in Figure 3 a high resolution excitation spectrum of that part of the K(D2) line which starts from the higher hyperfine level in the electronic ground state K($4s$, $F = 2$) and consists of three, partially overlapping contributions due to the K*($4p_{3/2}$, $F' = 1, 2, 3$) upper hyperfine levels.

The spectrum was obtained with a linearly-polarized single-mode laser (λ_1 = 766.7 nm) with an intensity of about 2 mW cm^{-2} and a linearly-polarized photoionization laser at λ_2 = 453 nm with a power of 60 mW (angle between polarization planes chosen to be 54.7°, ensuring independence of the photoionization signal of the intensity-dependent alignment in the intermediate state). The observed linewidth, somewhat broadened by saturation effects and — to a lesser extent — by the Doppler

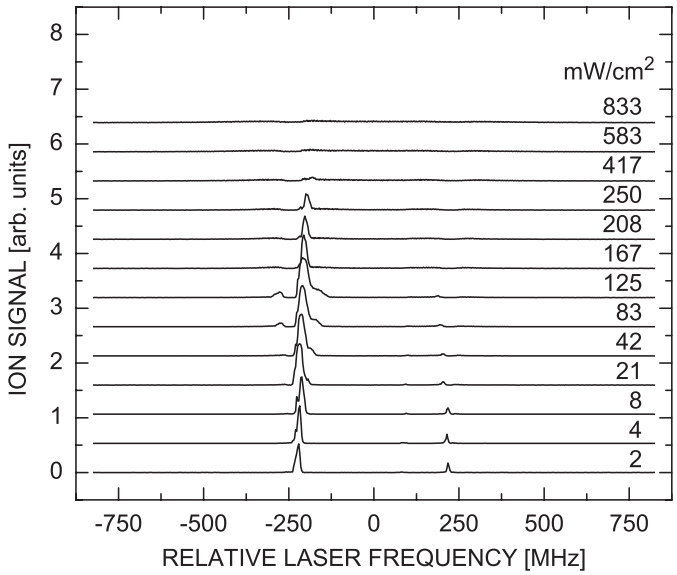

Fig. 4. Intensity dependence of the photoionization signal for the case of single mode excitation of the ^{39}K($4s\ ^2S_{1/2}$, $F = 1, 2 \rightarrow 4p\ ^2P_{3/2}$, F') transitions. The frequency f_L of the excitation laser is scanned around $f_0 = (f_{12} + f_{23})/2$; the frequency and intensity of the ionization laser are kept constant throughout.

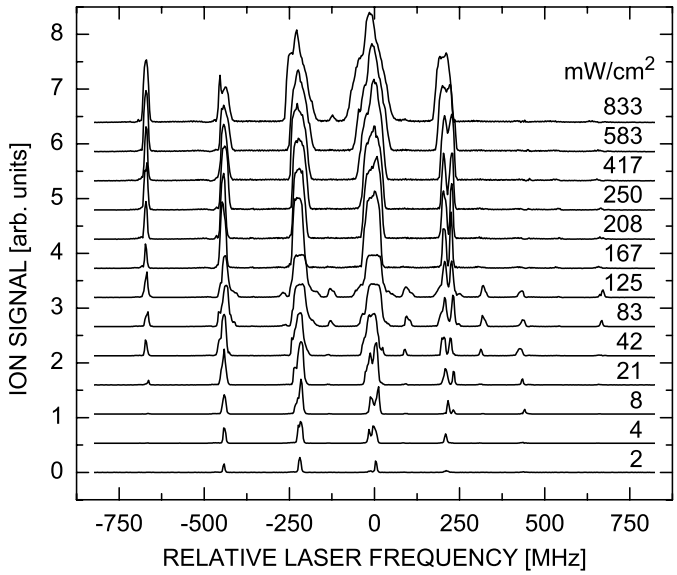

Fig. 5. Intensity dependence of the photoionization signal when the EO modulated laser is used to excite the ^{39}K($4s\ ^2S_{1/2}$, $F = 1, 2 \rightarrow 4p\ ^2P_{3/2}$, F') transitions. The frequency f_L of the Ti:Sa laser is scanned around $f_0 = (f_{12} + f_{23})/2$; the frequency and intensity of the ionization laser are kept constant.

effect, amounts to 10 MHz (FWHM). Under these conditions, the main component (frequency f_{23}) is rather well separated from the other two overlapping components f_{22} and f_{21}. It is clear, however, that the higher frequency wings in the Voigt profiles of the components f_{22} and f_{21} still have a significant excitation probability, especially when a higher intensity laser, stabilized onto the frequency f_{23} of the main component, is used to excite the atomic beam. As a consequence hyperfine pumping occurs due to spontaneous decay of the excited K*($4p\ ^2P_{3/2}$, $F' = 1, 2$) atoms to the lower K($4s\ ^2S_{1/2}$, $F = 1$) hyperfine level (see also [17]).

This effect is clearly demonstrated in experiments in which the intensity of the excitation laser is varied over the range 2–833 mW cm^{-2} (Fig. 4). Note that the result of this type of experiment will depend on the chosen geometry and laser beam diameters. In our case, the excitation laser and the ionization were anticollinear about a common axis with respective waist radii of about 1.5 mm and 0.5 mm. The photoion current is observed to saturate at rather low intensities and to strongly decrease at higher intensities. This behaviour reflects the fact that at higher laser intensities optical hyperfine pumping in the outer region of the excitation laser (i.e. before the atoms reach the region of the ionization laser) completely transfers the K($4s$, $F = 2$) population to the lower (unpumped) K($4s, F = 1$) level by spontaneous emission from the K*($4p_{3/2}$, $F' = 1, 2$) levels.

In a second series of experiments, we used an electrooptically modulated laser beam ($f_{EOM} = 220.35$ MHz). The phase-modulation is achieved by single passage through a $LiTaO_3$ crystal ($3\times3\times25$ mm^3) which is subjected to high electric field amplitudes. The latter are realized by using a resonance circuit (driven by an external oscillator at f_{EOM} to which the resonance circuit is inductively coupled) in which the crystal serves as the dielectric medium of the capacitor formed by two opposite, gold-plated surfaces (3×25 mm^2) of the crystal in appropriate cut and along the r_{33} direction [24]. Thus a high modulation index (around 1.84) is achieved such that the intensities of the first sidebands each carry almost a third of the intensity while the carrier frequency f_0 and the second sidebands each carry about 10% of the intensity. Using this EO-modulated laser beam, the excitation spectra shown in Figure 5 were obtained in which the total laser intensity (summed over all frequency components) was again varied over the range 2–833 mW cm^{-2}.

In contrast to the results shown in Figure 4, the density of excited potassium atoms in the ionization region is found to increase continuously with rising intensity of the excitation laser. At higher intensities, the effects of saturation become clearly visible through line broadening and little further increase in the ionization signal. Above about 400 mW cm^{-2} the peak intensity is nearly constant, indicating that essentially half of the atoms reside in the excited ^{39}K($4p_{3/2}$) level. The EO-modulated laser is thus proven to be well suited for efficient D2-line excitation of a collimated beam of potassium atoms.

4 Laser stabilization involving crossover saturation spectroscopy

In this section, we show how a single-mode laser (frequency f_L), from which a (predominantly) two-frequency

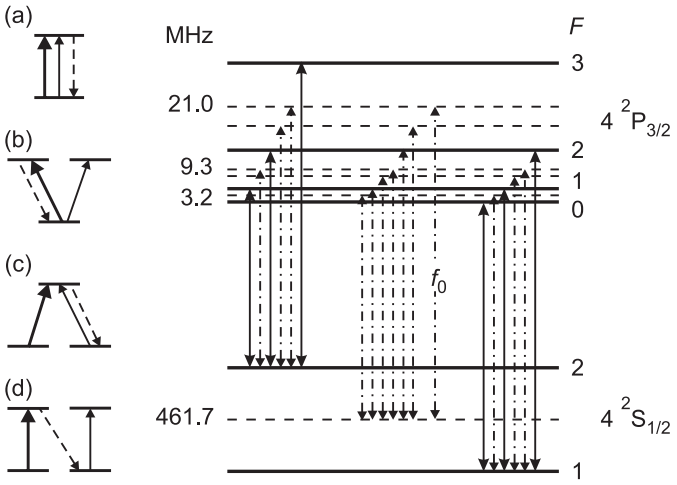

Fig. 6. Left side: illustration of the different types of crossover resonances. (a) I-type two level resonance. (b) V-type three level resonance. (c) Λ-type three level resonance. (d) N-type four level resonance. The thick and thin full arrows represent the pump and probe transition, respectively, the broken arrows denote spontaneous emission. In the crossover resonances (b), (c), and (d) the pump and probe transitions may be interchanged. Right side: transition diagram for ^{39}K($4s\ ^2S_{1/2}$, $F = 1, 2 \rightarrow 4p\ ^2P_{3/2}$, F'), illustrating the allowed hyperfine transitions (full arrows) and the crossover transitions (chain arrows). The numbers in the left column indicate the energy separations [MHz] between adjacent F-levels (full, thick lines).

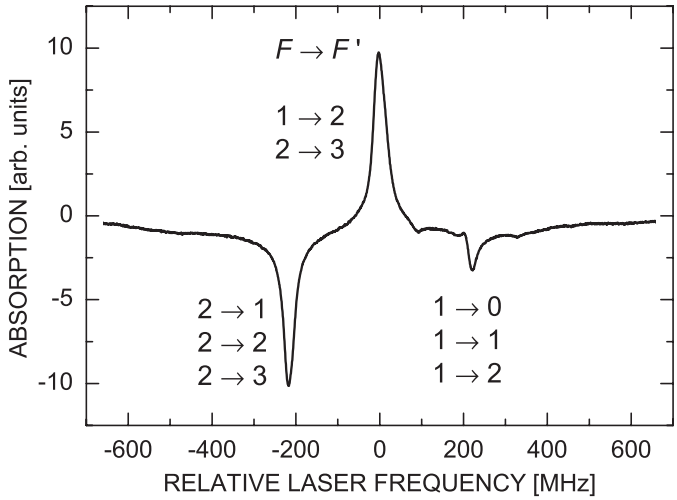

Fig. 7. Doppler-free saturation spectrum of the ^{39}K($4s\ ^2S_{1/2}$, $F = 1, 2 \rightarrow 4p\ ^2P_{3/2}$, F') transitions when the Ti:Sa laser is scanned around $f_0 = (f_{12} + f_{23})/2$.

spectrum is derived by electrooptical modulation, can be long-term stabilized to the proper frequency $f_0 = (f_{12} + f_{23})/2$ by exploiting a crossover resonance in the Doppler-free saturation spectrum of the ^{39}K(D2) line. Let us briefly recall the origin of the so-called crossover peaks (or dips) in saturated absorption spectroscopy [5] with anticollinear pump and probe laser beams which are assumed to have identical frequencies in the laboratory frame. When the saturating pump laser (thick full arrow) and the probe laser (thin full arrow) are both resonant with the relevant atomic transitions, four different types of resonances exist as illustrated in Figure 6: (a) I-type resonance (pump and probe laser address the same lower and upper levels); (b) V-type crossover (pump and probe laser address different upper levels); (c) Λ-type crossover involving different lower levels; (d) N-type four level crossover. Note that the pump and probe laser may be interchanged in the crossover schemes (b), (c), and (d).

In many cases of practical interest, the shown crossover resonances concern energetically nondegenerate atomic levels with the respective resonance conditions being introduced through the (first order) Doppler effect. As an example, assume that in the scheme (b) the two upper levels are separated by a frequency interval f_s which is well within the Doppler width δf_D of the considered transition which we assume to have an average transition frequency f_t (i.e. the two transitions in the atomic rest frame have the frequencies $f_\pm = f_t \pm f_s/2$). Assume now that the laser is tuned to the average transition frequency (i.e. $f_L = f_t$). Then both the pump and the probe laser are resonant with a special group of atoms whose velocity component along the direction of either probe or pump laser produces a Doppler shift of absolute size $f_s/2$. Under these conditions a reduced, velocity selective absorption occurs for the probe laser due to the action of the pump laser, and thus a crossover-peak arises in the saturated absorption spectrum for $f_L = f_t$. In case (c), on the other hand, the action of the pump-laser in combination with a sufficiently strong fluorescence (broken arrow) to the non-degenerate lower level can produce a velocity-selective dip in the saturated absorption spectrum of the probe laser when $f_L = f_t$.

In Figure 6 (right side), we summarize the resonant transitions (full arrows) and the crossover resonances (chain arrows) for the K(D2) line. Note the (middle) group of seven crossover resonances which are located at or close to the frequency $f_0 = (f_{12} + f_{23})/2$: they compose the crossover peak observed in the middle of the Doppler-free saturated absorption spectrum of the K(D2) line shown in Figure 7. The resonant transitions and crossover resonances, originating from the K($4s$, $F = 2$) and the lower-lying K($4s$, $F = 1$) hyperfine level, compose the left and right dips in the saturated absorption spectrum. The spectrum was taken with the saturation spectroscopic set-up sketched in Figure 2, using identical AOM frequencies for the first and second AOM. The zero of the frequency scale in Figure 7 corresponds to the maximum position of the crossover peak ($f_L = f_{CM}$). Note that the frequency $f_0 = (f_{12} + f_{23})/2$, to which the laser has to be long-term stabilized for optimal excitation efficiency, is located above that of the maximum of the crossover peak ($f_0 = f_{CM} + \Delta f$) by an amount $\Delta f \approx 15$ MHz.

Long-term stabilization of the single mode Ti:Sa laser to the relevant frequency f_0 is realized by frequency-offset locking onto the maximum of the crossover peak in which the frequency of the probe laser f_{pr} is identical with f_0. In this scheme the second AOM is driven at 110 MHz, i.e. the difference between the probe and pump laser

frequencies amounts to $f_{pr} - f_{pu} = 30$ MHz $= 2\Delta f$. Given this relation, Doppler free saturation peaks with nominal frequency f_n occur when the probe laser is tuned to $f_{pr} = f_n + \Delta f$. Thus, when the probe laser is tuned to the frequency f_0 we have $f_0 = f_n + \Delta f$, and this equation is fulfilled when f_n coincides with f_{CM} (see above). The actual stabilization is achieved by frequency modulation of the second AOM (frequency excursion about 30 MHz at a repetition rate of 3–5 kHz), yielding the derivative of the saturation spectrum around the maximum of the crossover peak which is sampled by phase-sensitive synchronous detection with a lock-in amplifier. The output of the lock-in amplifier provides the error signal which is fed back into the frequency stabilization loop involving a PID controller. We did not carry out a detailed analysis of the error signals, but we found the stabilization scheme (with the set-up mounted on a good optical table and under a flow box) to be very reliable and robust under normal laboratory conditions. The laser was thus fixed to the frequency f_0 to within the estimated short term fluctuations of about ± 1 MHz and without mode-hops over experimental periods of 10–20 hours. The typical long-time stability of the photoionization signal, which is the quantity of major concern in the practical use of the described excitation-ionization scheme in a laser photoelectron source (see Sect. 5), was around $\pm 3\%$ over several hours at sampling periods of a few seconds. These variations are attributed to fluctuations and drifts in the atomic potassium density and in the intensity of the photoionization laser.

5 Conclusions and perspectives

We have presented a reliable scheme for efficient long-term laser excitation of the potassium D2 line over long periods of time. It combines stabilization of a single mode laser with frequency $f_0 = (f_{12} + f_{23})/2$ onto a crossover peak in the Doppler-free saturation spectrum of the ^{39}K(D2) line with simultaneous excitation of the two transitions $^{39}\mathrm{K}(4s\ ^2\mathrm{S}_{1/2},\ F = 1 \rightarrow 4p\ ^2\mathrm{P}_{3/2},\ F' = 2)$ (frequency f_{12}) and $^{39}\mathrm{K}(4s\ ^2\mathrm{S}_{1/2},\ F = 2 \rightarrow 4p\ ^2\mathrm{P}_{3/2},\ F' = 3)$ (frequency f_{23}) by the first order sidebands $f_\pm = f_0 \pm f_{EOM}$ of the laser (f_0), generated by its electrooptical modulation at the frequency $f_{EOM} = (f_{12} - f_{23})/2$. In this way stable excitation of the two transitions on their proper frequencies is achieved and hyperfine pumping compensated over long periods of time. With appropriately adapted EOM frequencies, the described crossover stabilization and two-frequency excitation scheme can also be applied for efficient long-time excitation of Li and Na beams on the respective D2 line.

We have applied the described excitation and stabilization scheme to measurements of the absolute photoionization cross-section for (polarized) laser-excited $\mathrm{K}^*(4p_{3/2})$ atoms at photoelectron energies from threshold to 0.91 eV [30]. Taking advantage of the alignment of the laser-excited state we have determined the ratio of the electric dipole matrix elements D_d/D_s for ionizing the excited $4p$ electron into the d electron wave (D_d) and into the s electron wave (D_s), respectively [30]. These experiments will be described in more detail in a future paper.

The two-step excitation-ionization scheme illustrated in Figure 1 has also been applied to realize a source of monoenergetic photoelectrons for use in electron attachment [15,32,33] and electron scattering experiments [34]. In the attachment experiments we produce energy variable electrons (0–225 meV) by tuning the ionizing laser from 455 nm to shorter wavelengths (down to about 420 nm) with a birefringent filter (laser bandwidth about 0.15 meV). The electrons interact with molecules or clusters in the very same region where they are created, and the negative ions formed in electron attachment processes are analyzed with a quadrupole mass spectrometer and detected with an electron multiplier. In the scattering experiments, we produce very slow electrons by ionizing very close to threshold with a focussed laser of reduced bandwidth (0.05 eV) and extract the electrons with a constant electric field of about 10 V m^{-1} (which leads to a minimal energy width around 1 meV). Some results from these two types of experiments may be found in [15,32–34].

This work has been supported by the Deutsche Forschungsgemeinschaft, by the EU through the HCM programme (LAMBDA network), and by the Zentrum für Lasermesstechnik und Diagnostik. We thank A. Schramm and H. Wenz for helpful discussions and K. Zinsmeister for technical support.

References

1. I.V. Hertel, W. Stoll, Adv. At. Mol. Phys. **13**, 113 (1978)
2. K. Bergmann, in *Atomic and Molecular Beam Methods*, edited by G. Scoles (Oxford Univ. Press, New York and Oxford, 1988), Vol. 1, p. 239
3. W.R. MacGillivray, M.C. Standage, Phys. Rep. **168**, 1 (1988)
4. J.J. McClelland, in *Experimental Methods in the Physical Sciences* (Academic Press, San Diego, CA, USA, 1996), Vol. 29B, p. 145
5. W. Demtröder, *Laser Spectroscopy,* 2nd edn. (Springer, Heidelberg, New York, 1998)
6. M. Zhu, J.L. Hall, in *Experimental Methods in the Physical* Sciences (Academic Press, San Diego, CA, USA, 1997), Vol. 29C, p. 103
7. B.G. Lindsay, K.A. Smith, F.B. Dunning, Rev. Sci. Instrum. **62**, 1656 (1981)
8. B. Chéron, H. Gilles, J. Hamel, O. Moreau, H. Sorel, Phys. III France **4**, 401 (1994)
9. K.L. Corwin, Z.-T. Lu, C.F. Hand, R.J. Epstein, C.E. Wieman, Appl. Opt. **37**, 3295 (1998)
10. V.V. Yashchuk, D. Budker, J.R. Davis, Rev. Sci. Instrum. **71**, 341 (2000)
11. W. Jitschin, Appl. Phys. B **33**, 7 (1984)
12. H.A.J. Meijer, H.P. van der Meulen, F. Ditewig, C.J. Wisman, R. Morgenstern, J. Phys. E **20**, 305 (1987)
13. K. Harth, M. Raab, H. Hotop, Z. Phys. D **7**, 213 (1987)
14. T. Kraft, M.-W. Ruf, H. Hotop, Z. Phys. D **14**, 179 (1989)
15. J.M. Weber, E. Leber, M.-W. Ruf, H. Hotop, Eur. Phys. J. D **7**, 587 (1999)

16. E. Arimondo, M. Inguscio, P. Violino, Rev. Mod. Phys. **49**, 31 (1977)
17. L. Brencher, B. Nawracala, H. Pauly, Z. Phys. D **10**, 211 (1988)
18. W. Dreves, W. Kamke, W. Broermann, D. Fick, Z. Phys. A **303**, 203 (1981)
19. I.V. Hertel, A.S. Stamatovic, IEEE J. Quant. Electron. **11**, 210 (1975)
20. E.E.B. Campbell, H. Hülser, R. Witte, I.V. Hertel, Z. Phys. D **16**, 21 (1990)
21. G. Baum, C.D. Caldwell, W. Schröder, Appl. Phys. **21**, 121 (1980)
22. S.R. Lorentz, R.E. Scholten, J.J. McClelland, R.J. Celotta, Phys. Rev. A **47**, 3000 (1993)
23. W. Ertmer, R. Blatt, J.L. Hall, M. Zhu, Phys. Rev. Lett. **54**, 996 (1985)
24. J.F. Kelly, A. Gallagher, Rev. Sci. Instrum. **58**, 563 (1987)
25. X.L. Han, G.W. Schinn, A. Gallagher, Phys. Rev. A **38**, 535 (1988)
26. H. Reich, H.J. Jänsch, Nucl. Instrum. Meth. Phys. Res. A **288**, 349 (1990)
27. U. Müller, H.A.J. Meijer, N.C.R. Holme, M. Kmit, J.H.V. Lauritsen, J.O.P. Pedersen, C. Richter, J.W. Thomsen, N. Andersen, S.E. Nielsen, Z. Phys. D **33**, 187 (1995)
28. V. Karaganov, I. Bray, P.J.O. Teubner, J. Phys. B **31**, L187 (1998)
29. K.A. Stockman, V. Karaganov, I. Bray, P.J.O. Teubner, J. Phys. B **31**, L867 (1998)
30. I.D. Petrov, V.L. Sukhorukov, E. Leber, H. Hotop, Eur. Phys. J. D **10**, 53 (2000)
31. P.C.D. Hobbs, Opt. Phot. News, 17 (April 1991)
32. J.M. Weber, E. Leber, M.-W. Ruf, H. Hotop, Phys. Rev. Lett. **82**, 516 (1999)
33. H. Hotop, M.-W. Ruf, M. Allan, I.I. Fabrikant, Adv. At. Mol. Opt. Phys. **49**, 85 (2003)
34. A. Gopalan, J. Bömmels, S. Götte, A. Landwehr, K. Franz, M.-W. Ruf, H. Hotop, K. Bartschat, Eur. Phys. J. D **22**, 17 (2003)